ELSEVIER

Colloids and Surfaces
A: Physicochemical and Engineering Aspects 151 (1999) 311–320

COLLOIDS AND SURFACES A

# Porous carbon from polymer waste materials

Krisztina László [a,*], Attila Bóta [a], Lajos György Nagy [a], Israel Cabasso [b]

[a] *Department of Physical Chemistry, Technical University Budapest, Budapest, H-1521, Hungary*
[b] *Polymer Research Institute Chemistry Department, State University of New York, College of Environmental Science and Forestry, Syracuse, NY 13210, USA*

Received 4 November 1997; accepted 11 March 1998

**Abstract**

Polymer waste materials, instead of ending up in incineration plants, can better be recycled into activated carbon. The properties of polyacrylonitrile, polyethyleneterephthalate and cellulose based carbons prepared by steam activation are reported in this paper. Microscopic (SEM, STM or AFM), SAXS and various adsorption techniques have been applied to describe the matrix and surface characteristics. These polymer based carbons can be characterized by a well developed pore structure. Their specific surface area ($S_{BET}$) proved to be 540–1250 $m^2/g$. Their surface is polar enough to adsorb phenol from aqueous solution, resembling commercial activated carbon which is sold for waste water treatment. 

*Keywords:* Activated carbon; Cellulose; Microstructure; Phenol adsorption; Polyacrylonitrile; Polyethyleneterephthalate

## 1. Introduction

The industrial treatment of durable polymer waste in the form of plastics, rubbers, and foams, that consist of a high carbon fraction, often end up in incineration plants. This type of waste can, however, better be recycled into activated carbon products that can be applied for further environmental pollution treatment (Fig. 1).

Carbon material is formed by pyrolyzing polymers at very high temperatures in a non-oxidative environment. Activated carbons for waste water treatment, air purification and industrial use are produced from naturally occurring raw material, such as coal, oil, peat, wood and other sources of high carbon content [1,2]. Most of these are polymers, including agricultural products that have been developed as superior active carbons, especially fruit piths and hard shells [3–8]. It is well established that other polymers can be a source of carbon. Thermal degradation properties of polyacrylonitrile and extracted cellulose are well documented [9–22], especially the polyacrylonitrile pyrolysis product that has been well characterized in recent decades for the production of carbon fibers.

The objective of this article is to show that some important polymer waste materials can be used for production of activated carbons. However, many materials that are of potential interest can be carbonized. Three examples of these are: polyethyleneterepthalate (PET), a polymer that was developed to replace glass in soft drinks bottles and containers; cellulose for paper and packing materials; and polyacrylonitrile copolymers (PAN) used in the production of synthetic fabrics.

* Corresponding author. Fax: +36 1463 3519;
e-mail: klaszlo@ch.bme.hu

0927-7757/99/$ – see front matter 
PII S0927-7757(98)00390-2

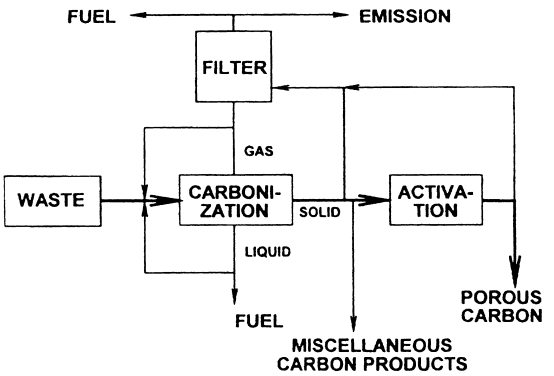


Fig. 1. Scheme of polymer recycling.

In this communication we want to report on the properties of activated carbon from these three polymers, namely morphology, matrix and pore structure and chemical character of the surface. Also, the results of preliminary experiments as to their potential adsorption of solutes from aqueous phenol solutions. The versatile adsorption properties of microporous carbons derive from their complex structure [23–25]. Within these microporous carbons the basic structural units are graphitic crystallites, amorphous carbon and inorganic impurities. The complex structure develops during the preparation process and might be influenced by the combination of heat treatment and activation steps [26–31]. Besides, the chemical composition and structural behavior of the raw material play a significant role in the character of the resulting carbon [1,3,4,32–34]. In the case of phytogenic precursors or organic polymers the semicrystalline structure develops during the heat treatment. The sizes of the microcrystallites and the pores are interrelated and very often show similar values [35]. The surface functionalities developing during the heat treatment and activation also influence the adsorption properties [36–40]. Therefore, the matrix, the pore structure and the chemical character of the surface determine the adsorption capability of the carbon.

## 2. Methods of approach

Many methods are described in the literature to characterize carbon and activated carbon. Some of them are dubious in the opinion of the authors, for example most of the IR information that has been reported, especially before 1990 for carbons that were prepared at high temperatures ($\leqslant 800^{\circ}C$). In this study several methods were used for the characterization of the three activated carbon samples.

A microscopic picture provides visual information on the structure of the surfaces. Scanning electron microscopy can be used in the micrometer range, and with an atomic force microscope (AFM) we can reach the nanosize region of the probes.

The pore and matrix structure, however, can be simultaneously studied by the small angle X-ray scattering (SAXS) method [41,42]. Activated carbon also scatters the traversing X-ray beam in the small angle regime, because the electron density shows inhomogeneity in the colloidal region [43]. The primary structural parameter generally obtained from SAXS results is the Guinier radius which can only be calculated and interpreted under strict conditions. A modified approach of the Guinier formula has been applied in this paper.

Porous adsorbents are most often characterized by the low temperature nitrogen adsorption method [44,45]. The analysis of the nitrogen adsorption isotherms according to the various adsorption theories in different ranges of relative pressure provides information not only on the specific surface area of the adsorbents but also on the pore size in the micro- and mesopore range.

The chemical surface groups are most often determined by titration according to Boehm and coworkers [46,47], different IR techniques [48], or, as an overall feature, by applying an adequate binary liquid mixture for adsorption [49–54].

The adsorption capacity of a particular activated carbon in a purification process is best determined experimentally with the contaminant molecule(s) in question, as there are too many independent and interrelating parameters influencing the adsorption performance. An important feature for waste water treatment is the phenol adsorption capacity of a carbon, as this molecule is one of the most frequently occurring contaminants in industrial waste waters [55]. It is not only carcinogenic but gives a bad taste and odor even in low

concentrations. Its $pK_{20\circ C}$ is 9.89 [56]. Phenol is a relatively small molecule (its cross-sectional area is 41–0.55 $Å^2$/molecule in the flat position, i.e. the diameter is ca. 8 Å) [57,58]. Phenol molecules in aqueous solutions are able to completely fill the micropore volume at saturation [59]. Nevertheless, it was found recently that the presence of acidic surface functional groups hinders the ability of activated carbon to adsorb phenolic compounds in the presence of dissolved oxygen by reducing its effectiveness in promoting adsorption via oxidative coupling reactions [60].

## 3. Experimental

### 3.1. Preparation of the samples

The polyacrylonitrile fiber was provided from Zoltek-Hungarian Viscosa Ltd. (Hungary). The granulated polyethyleneterephthalate (Qualon) was obtained from Mitsubishi (Singapore). Packing paper was used as a source of cellulose. The raw material was carbonized at 700°C in a steel reactor flushed with nitrogen gas (50 $dm^3$/h). The carbonized char samples were activated in a steam flow of 18 g/h at 900°C in a rotary quartz reactor [61]. The steam was diluted with nitrogen in a molar ratio of 1:1. The time of activation was optimized in order to obtain a burn-off of 50% related to the mass of the char. It took 45 min in the case of the cellulose and polyacrylonitrile precursors and 90 min in the case of the polyethyleneterephthalate preparation process.

### 3.2. Methods

Scanning electron microscopic pictures were taken with an Etec Autoscan microscope (USA). The accelerating voltage applied was 20 kV and the working distance was optimized at 20–24 mm. Magnification is given in the figures.

AFM pictures were taken with a Nanoscope III (Digital Instrument) microscope.

The SAXS measurements were performed by a Kratky camera and a proportional counter (Anton Paar, Graz, Austria). The scattering of Ni-filtered Cu Kα radiation ($\lambda = 1.542$ Å) was recorded in the $6 \times 10^{-3}$–0.6 $Å^{-1}$ range of the scattering variable, defined as $h = (4\pi \sin \Theta)/\lambda$, where $2\Theta$ and $\lambda$ are the scattering angle and the wavelength, respectively. The primary beam was line focused. The intensity curves were corrected considering the geometry of the beam profile in order to obtain point-focused curves.

The nitrogen adsorption/desorption isotherms were measured at the boiling point of liquid nitrogen (77 K) from $p/p_0 \approx 0.004$ with an AUTOSORB (Quantachrome, Syosset, NY, USA) computer controlled surface analyser. Samples were outgassed at 400°C in high vacuum ($p < 5 \times 10^{-7}$ torr). The specific surface area and the pore size distribution were derived from the isotherms [62].

Adsorption from benzene (1)–methanol (2) binary liquid mixtures was measured in order to characterize the chemical heterogeneity of the carbon surfaces. Isotherms were measured by a batchwise method [63] in the whole composition range at ambient temperature. The applied solid/liquid ratio was 1:5. The contact time from preliminary experiments was 6 h. The concentrations were derived from the refractive index measured by interferometer.

Adsorption isotherms with aqueous phenol solutions were determined at 20°C under static conditions by the batchwise multisample method [64]. Aqueous solutions with different initial concentrations were used. The pH was not buffered and was nearly neutral in all cases ($7.0 \pm 0.5$). Stoppered flasks containing the adsorbent and the adsorbate in solution (solid/liquid ratio $\approx 0.1$ g/100 $cm^3$) were shaken in a thermostatic bath for 24 h. The contact time was established in preliminary kinetic experiments. The concentration of phenol in the aqueous solutions was determined spectrophotometrically at a wavelength of 254 nm, using a UVIKON 930 UV/visible spectrophotometer (Kontron, Zurich, Switzerland).

## 4. Results and discussion

### 4.1. Microscopic characterization

According to the SEM pictures of the activated probes (Fig. 2), their structure on the few-microm-

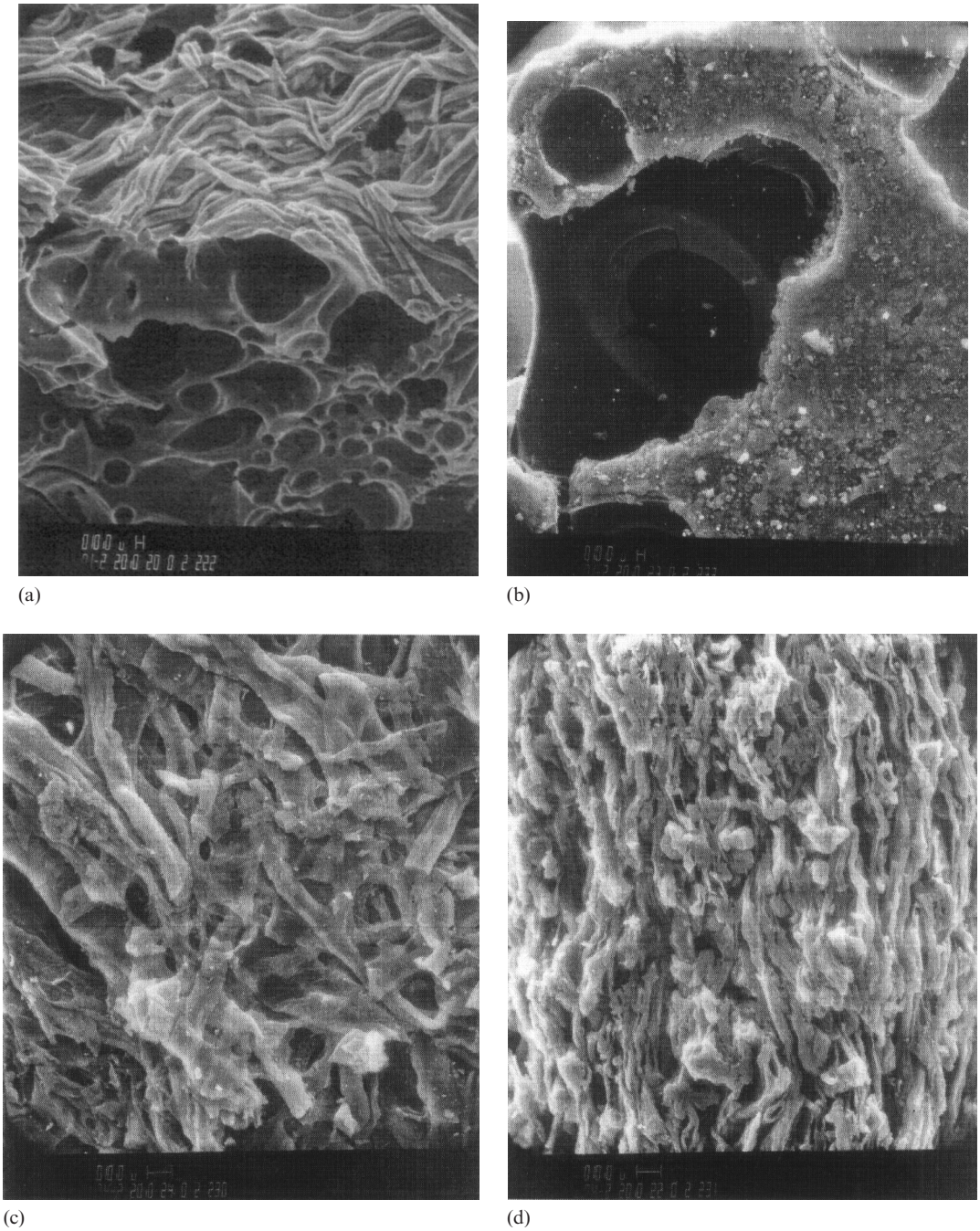

(a) (b)

(c) (d)

Fig. 2. seM picture of activated polymers. (a) PAN carbon, the magnification is 100, the bar below the picture means 10 μm; (b) PET carbon, the magnification is 100, the bar below the picture means 10 μm; (c) surface of cellulose carbon, the magnification is 400, the bar below the picture means 10 μm; (d) cross-section of cellulose carbon, the magnification is 400, the bar below the picture means 10 μm.

eter level reminds us of the structure of the precursor. The fibers can be clearly distinguished in the case of the PAN derived carbon, though as the fibers become melted and stuck together the solidified bubbles blown by the evolving gases can be recognized in the probe [Fig. 2(a)]. The gas evolving at elevated temperature blows holes into the molten, originally granular PET polymer, while the heat treatment and the activation strongly erode the previously smooth surface [Fig. 2(b)]. The fibrous character of the cellulose shows in both the vertical and horizontal cutting of the cellulose based carbon, reflecting both the remains of the phytogenic structure [5] and the way in which the cellulose paper was made in the pulp filtration step during its manufacture [Fig. 2(c,d)].

According to STM pictures reported recently [65], the PET derived sample consists of closely packed parallel anisotropic units of about 5000 Å in length and 1000 Å in diameter, having a finer arrangement with a thickness of 200–300 Å along these units. Better resolution shows that the surface consists of isotropic units with a diameter of 10–30 Å. Cellulose based carbon is also made of about 1000 Å thick units, but their length is varied. The fibrous units form a loose, irregular network as a result of the complex phytogenic precursor structure. A 200–300 Å pattern can be observed along the fibers as well. At higher resolution this probe shows a heterodispersive size distribution, i.e. no further structural details can be recognized. In the AFM picture of the PAN based sample [$1 \times 1\ \mu m^2$, Fig. 3(a)] a layered pattern of 2000–5000 Å can be distinguished, built up of layers with a thickness of about 250 Å. According to higher resolution pictures ($200 \times 200\ nm^2$), the surface is covered by 20–30 Å size disperse units [Fig. 3(b)].

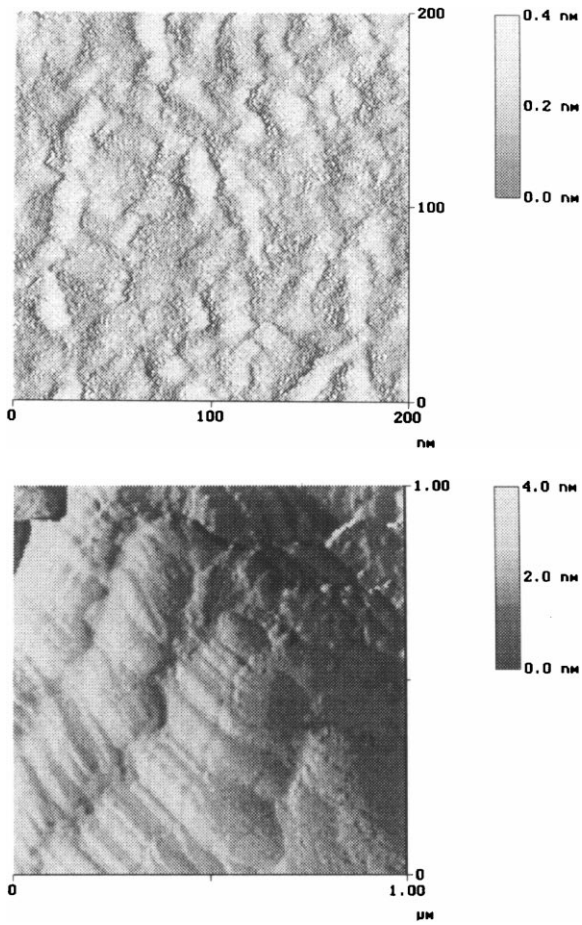


Fig. 3. AFM picture of PAN derived carbon at lower (a) and higher (b) resolution.

### 4.2. SAXS characterization

Due to their heterogeneous matrix structure, all three samples show scattering in the small angle region. None of the samples gave a linear initial plot in the $\log I$ vs. $h^2$ representation because of their heterodispersive size distribution. Therefore, instead of the Guinier plot, the approach described by Shull and Roess [66] was applied. The distribu-

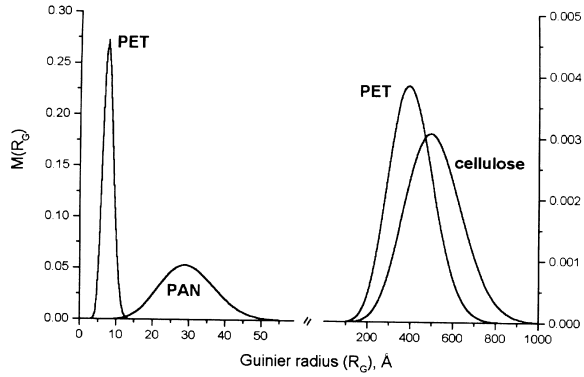


Fig. 4. Guinier radius distribution of activated polymer carbons.

tion of the Guinier radii is shown in Fig. 4. The PAN and cellulose derived samples have one, the PET derived sample has two characteristic distribution peaks, providing size and dispersity data which are comparable with the earlier mentioned STM and AFM observations. Assuming that the particles resulting in the peaks in the larger $R_G$ range are narrow cylinders, their characteristic diameter calculated as $2R_{cylinder}=2(\sqrt{4/3})R_G$ proved to be 900 and 1160 Å for the PET and the cellulose derived carbon, respectively. From the shape of the peaks the more heterodisperse character of the cellulose–carbon is obvious. The PET carbon shows a second peak in the smaller $R_G$ region as well, with a maximal value of 7.6 Å. The absence of a second cellulose–carbon peak in this regime is not surprising as it did not show any size limit in the STM picture either [65]. The single peak of the PAN derived carbon is shown in this range. The maximum value of this wide distribution curve is 29.1 Å. Assuming spherical particles, from the $2R=2(\sqrt{5/3})R_G$ equation the average diameter of PET and PAN based carbons is 20 and 75 Å, respectively. The size of these smaller carbon units is in good agreement with the 10–30 Å size isotropic units in the STM pictures. At the same time, the diameter of 75 Å is more than double the size observed by AFM in the case of the PAN derived carbon. The reason for the deviation might be that the size of the particles is significantly smaller on the surface of this carbon than in its bulk phase. Another explanation is that the PAN derived carbon is compact and does not consist of individual scattering units, i.e. the conditions of the Guinier model are not fulfilled.

### 4.3. Pore structure from $N_2$ adsorption

The pore structure of the carbons was characterized by using the nitrogen adsorption–desorption isotherms (Fig. 5). The isotherms of cellulose derived carbon are of type IV according to the IUPAC classification with hysteresis loop [67]. The isotherm of PAN and PET based activated carbon practically belongs to the Langmuir type. PET carbon has a hysteresis loop, which can hardly be detected in the case of the PAN carbon

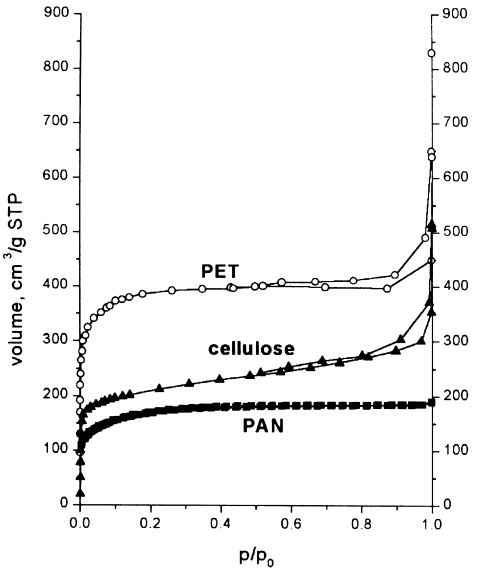


Fig. 5. Low temperature $N_2$ adsorption isotherms. Symbols represent measured points.

(Fig. 5). In the cases of these two carbons the saturation value is almost reached by $p/p_0=0.2$. As the adsorption in the low relative pressure range traces back to the presence of micropores, PAN and PET carbon mostly contains micropores, while the cellulose sample also contains mesopores in a considerable ratio. The contribution of the micropores is also reflected in the specific surface areas calculated according to the Brunauer, Emmett and Teller (BET) model ($S_{BET}$). The $S_{BET}$ values are 1254, 659 and 544 $m^2/g$ in the case of PET, cellulose and PAN based carbons, respectively.

The adsorption in the micropores was interpreted according to the pore filling model [68,69]. The two-term Dubinin–Radushkevich (D–R) equation was used [65,70] in the $0<p/p_0<0.2$ range:

$$W=W_1+W_2=W_{01}\exp\left[\left(-\frac{RT}{\beta E_1}\ln\frac{p_0}{p}\right)^2\right]+W_{02}\exp\left[\left(-\frac{RT}{\beta E_2}\ln\frac{p_0}{p}\right)^2\right] \quad (1)$$

where $E_1$ and $E_2$ are the adsorption energies, $W_{01}$ and $W_{02}$ are the volumes of the micropores and

$W$ is the volume of the partially filled micropores. $\beta=0.33$ was used for $N_2$ adsorption [65,71,72]. The characteristic micropore dimensions can be derived from these $E$ values by various semi-empirical equations [36,58,73–79]. The pore size distribution functions were derived according to the method of Spitzer et al. [74]. Their method is essentially a modified version of the D–R method:

$$dW/dr = W_0(k/E)^n(ns/r^{ns+1})\exp[-(k/E)^2 r^{-ns}] \quad (2)$$

where $r$ is the micropore radius, $k=0.695$ kJ nm$^3$/mol calculated from the Kirkwood–Müller equation for laterally ended pores and nitrogen–carbon interaction; $n=2$ according to the D–R equation and $s=3$ is the exponent of the pore radius in the de Boer–Custers equation [74,80,81]. The distribution function is calculated by using the relation $r \propto E^{1/s}$. The overall $dW/dr$ distribution functions are shown in Fig. 6 for all three samples (solid lines). The shapes of the three functions are similar, however, the PAN derived carbon has not only a shoulder, but two distinct peaks. After decomposition (broken lines) the average pore radii calculated for the two pore size ranges are 2.6 and 4.4 Å, 3.1 and 4.5 Å and 2.9 and 4.5 Å for PAN, PET and cellulose based carbons, respectively. The differential pore size distribution of the PAN carbon decreases very sharply, reaching the $x$-axis at $r<20$ Å. Both PET and cellulose based carbons exhibit a sharp peak at $r\sim20$ Å. None of the carbons shows further distribution peaks at higher radii in the mesopore range.

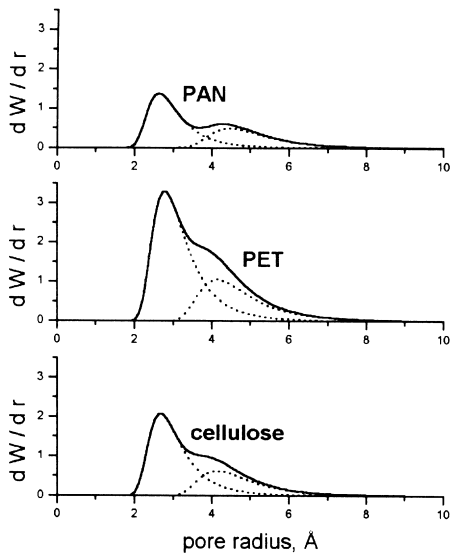


Fig. 6. Micropore size distribution from $N_2$ adsorption. Solid line: overall curves; broken line: decomposed curves.

### 4.4. Chemical character of the surface

The surface functional groups of carbon, especially oxygen containing ones, have a large impact on the adsorption of organic molecules from liquid phase, e.g from aqueous solutions. The adsorption from benzene–methanol binary liquid mixtures was used to describe the surface characteristics. Surface oxides impart polar character to carbons resulting in the preferential adsorption of the alcohol component of the binary mixture [82,83]. The interaction of the π-electrons of the benzene with the surface promotes the adsorption of the nonpolar component [84]. The carboxylic acid complexes on the carbon surface are responsible for the behavior in which both components of the binary mixture adsorb, rendering the surface both benzophilic and polar.

Excess isotherms ($n_1^{\sigma(n)}$ vs. $x_1$ functions) were calculated from the primary experimental data:

$$n_1^{\sigma(n)} \equiv n_0(x_{1,0}-x_1) = n^s x_1^s - n^s x_1 \quad (3)$$

where $n_1^{\sigma(n)}$ is the specific surface excess amount (mmol/g) of benzene in the interfacial layer, $n_0$ is the specific amount of the initial bulk liquid phase (mmol/g), $x_{1,0}$ and $x_1$ are the initial and the equilibrium molar fractions of the benzene, respectively, in the bulk phase. The specific amount of adsorbed liquid in the interfacial layer is designated $n^s$ and $x_1^s$ is its composition in equilibrium. When $0<x_1<1$ and $n_1^{\sigma(n)}=0$, $x_1^s=x_1=x_{1,a}$. This is the so called adsorption azeotropic composition, where the composition of the bulk and interfacial phases are equal. All three isotherms (Fig. 7) are of type IV according to the Schay–Nagy classification [85]. $x_{1,a}=0.68$, 0.62 and 0.67 in PAN, PET and cellulose derived samples, respectively. In the case of all the samples in the $0<x_1<x_{1,a}$ interval the nonpolar benzene adsorbs preferentially while in the $x_{1,a}<x_1<1$ range the adsorption of the

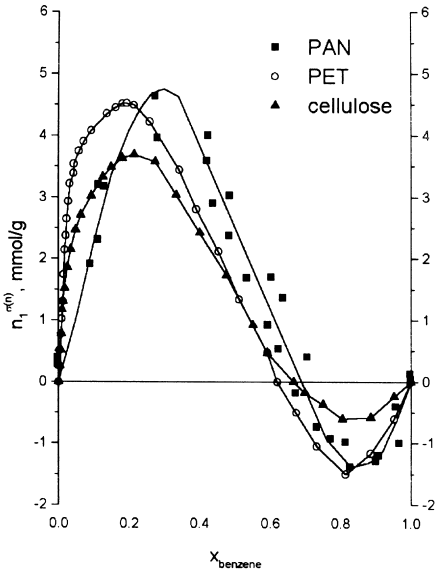


Fig. 7. Benzene (1)–methanol (2) excess adsorption isotherms of polymer based carbons.

polar methanol is preferred, showing that the surfaces contain both nonpolar and polar surface sites. All the isotherms have a relatively long linear section. In this bulk region the composition of the interfacial layer is practically constant [63,85–88] and equals $x_{1,a}$. As all three samples possess polar surface sites, they are potential adsorbents for organic pollutants dissolved in aqueous solution.

### 4.5. Adsorption test with aqueous phenol solution

Phenol adsorption isotherms of the polymer based carbons are shown in Fig. 8 together with the phenol uptake of F400, a commercial activated carbon (Calgon Carbon Corp., Pittsburg, PA, USA) produced for phenol removal. Its $S_{BET}$ is 926 $m^2$/g. Symbols represent measured data. Solid lines were fitted according to the Langmuir model, which obviously does not give the best fit in all cases. According to Gile's classification the adsorption isotherms are of type L in all cases except PAN derived carbon, which exhibits type H. Carbons giving an isotherm of type L are considered to have an excess of acidic surface groups [89]. H type isotherms mean the presence of a small number of very strong adsorption sites.

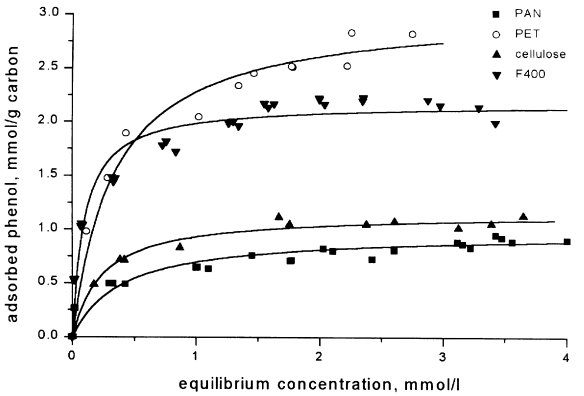


Fig. 8. Phenol uptake from aqueous solutions. Symbols represent measured data. Solid lines were fitted by the Langmuir equation.

The phenol adsorption capacities of the carbon samples prepared in our laboratories are comparable or even higher in the case of PET carbon than of the commercial one. The adsorption limits are 0.88, 2.56 and 1.06 mmol/g in the case of PAN, PET and cellulose carbons, respectively. The phenol uptake of F400 was found to be 2.23 mmol/g. The surface area occupied by a single phenol molecule was calculated and found to be 120 and 115 $Å^2$/molecule in the case of PAN and cellulose carbons, respectively. Significantly smaller values, 80 and 73 $Å^2$/molecule, were obtained for PET carbon and F400, respectively. All of these values are higher than the cross-sectional area of phenol (41–55 $Å^2$/molecule [91]). As the overall polarity, i.e. the $x_{1,a}$ values of the surfaces, are very similar, the polar/nonpolar character does not play a role in the dissimilarity of the surface phenol population. The reason is, in part, that phenol and water molecules compete for the adsorption sites of the surface. The fraction of the surface occupied by the solvent molecules is not considered in this calculation. At the same time, the critical size of phenol molecules is about 3.5 Å [90]. This value does not take into account the increased size of the dissolved phenol formed by the interaction with the solvent molecules. Nevertheless, pores below a limited size are not available for the phenol molecules. At the same time, part of these pores are accessible for the smaller $N_2$ molecules (its critical size is 3 Å) and thus included in $S_{BET}$. Therefore, part of the pores

reckoned within the first peak of the curves in Fig. 6 does not contribute to the phenol uptake.

## 5. Conclusion

Activated carbons of polymer waste origin can be converted to porous activated carbons. In spite of the high carbon content of the precursors, the porous structure developed during the preparation is strongly influenced by the original matrix structure of the polymers. The specific surface area, $S_{BET}$, achieved was 540–1250 $m^2/g$. According to phenol adsorption tests they exhibit pollutant uptake comparable to commercial carbon, although a part of the surface does not contribute to the phenol adsorption. Adsorption tests with further pollutant molecules of different size may support these results.

## Acknowledgment

The research described in this paper was supported by OTKA Funds (Hungary) No. T 017019 and T 017039. Credit is due to Mr. Han Liu for the SEM pictures and Mr. Thomas Copitzky for the AFM pictures. The authors wish to express their appreciation to Ms. Emese Fülöp, Mr. György Bosznai and Mr. Miklós Kövi for their experimental work.

## References

[1] T. Wigmans, Carbon 27 (1989) 13.
[2] J. Wilson, Fuel 60 (1981) 833.
[3] F. Rodriguez-Reinoso, M. Molina-Sabio, Carbon 30 (1992) 1111.
[4] K. Gergova, N. Petrov, S. Eser, Carbon 32 (1994) 693.
[5] M.G. Lussier, J.C. Shull, D.J. Miller, Carbon 32 (1994) 1493.
[6] M.T. Gonzáles, M. Molina-Sabio, F. Rodriguez-Reinoso, Carbon 32 (1994) 1407.
[7] L.H. Noszkó, A. Bóta, G. Pálinkás, L.G. Nagy, in: Proc. 4th Hungarian Conf. on Colloid Chemistry, Eger, Hungary, 1983, p. 272.
[8] A. Bóta, K. László, H. Schlimper, L.G. Nagy, ACH Mod. Chem. 134 (2–3) (1997) 169.
[9] R. Bilbao, J. Arauzo, A. Millera, Thermochim. Acta 120 (1987) 121.
[10] M. Lewin, A. Basch, B. Shaffer, Cell. Chem. Technol. 24 (1990) 417.
[11] T. Hirata, Nihon Mokuzai Gakkaishi 41 (1995) 879.
[12] I. Milosavljevic, V. Oja, E.M. Suuborg, Ind. Eng. Chem. Res. 35 (1996) 653.
[13] P.H. Wang, L.R. Yue, J. Liu, J. Appl. Polym. Sci. 60 (1996) 923.
[14] T.H. Ko, C.H. Lin, H.Y. Ting, J. Appl. Polym. Sci. 37 (1989) 553.
[15] E. Fitzer, Carbon 27 (1989) 621.
[16] G. Pan, N. Muto, M. Miyayama, H. Yanagida, J. Mater. Sci. 27 (1992) 3497.
[17] T. Usami, T. Hoh, H. Ohtani, S. Tsuge, Macromolecules 23 (1990) 2460.
[18] T.-H. Ko, J. Appl. Polym. Sci. 43 (1990) 589.
[19] E. Fitzer, W. Frohs, M. Heine, Carbon 24 (1986) 387.
[20] T.-H. Ko, P. Chiranairadue, C.-K. Lu, C.-H. Lin, Carbon 30 (1992) 647.
[21] L.H. Peebles, P. Peyser, A.W. Snow, W.C. Peters, Carbon 28 (1990) 707.
[22] A. Basch, M. Lewin, J. Polym. Sci. 11 (1973) 3071.
[23] M. Smisek, S. Cerny, in: Active Carbon, Elsevier, New York, 1970.
[24] R.C. Bansal, J.B. Donnet, F. Stoeckli, Active Carbon, Marcel Dekker, New York, 1988.
[25] M.M. Dubinin, in: P.L. Walker Jr. (Ed.), Chemistry and Physics of Carbon, vol. 2, Marcel Dekker, New York, 1968, chapter 2.
[26] U. Hofmann, D. Wilm, Z. Electrochem. 42 (1936) 504.
[27] B.E. Warren, Phys. Rev. 59 (1941) 693.
[28] M.M. Dubinin, in: S.J. Gregg, K.S.W. Sing, H.F. Stoeckli (Eds.), Characterisation of Porous Solids, Society of Chemical Industry, London, 1979, p. 1.
[29] M. Evans, H. Marsh, in: S.J. Gregg, K.S.W. Sing, H.F. Stoeckli (Eds.), Characterisation of Porous Solids, Society of Chemical Industry, London, 1979, p. 53.
[30] N. Setoyama, M. Ruike, T. Kasu, T. Suzuki, K. Kaneko, Langmuir 9 (1993) 2612.
[31] K. Kaneko, C. Ishii, H. Kuwabara, Carbon 30 (1992) 1075.
[32] A. Juhola, J. Kemia-Kemi 11 (1977) 543.
[33] A. Juhola, J. Kemia-Kemi 12 (1977) 653.
[34] T. Wigmans, in: A. Capelle, F. de Vooys (Eds.), Activated Carbon… A Fascinating Material, Norit N.V., Amersfoort, NL, 1983, p. 58.
[35] A. Bóta, J. Appl. Cryst. 24 (1991) 635.
[36] H.F. Stoeckli, Carbon 28 (1990) 1.
[37] J. Jagiello, J.A. Schwarz, Langmuir 9 (1993) 2513.
[38] T.J. Bandosz, J. Jagiello, J.A. Schwarz, Langmuir 9 (1993) 2518.
[39] H. Xijun, D.D. Duong, Langmuir 9 (1993) 2530.
[40] M. Heuchel, M. Jaroniec, R.K. Gilpin, P. Bräuer, M. v. Szombathely, Langmuir 9 (1993) 2537.
[41] A. Jánosi, H.F. Stoeckli, Carbon 17 (1979) 465.

[42] A. Bóta, K. László, L.G. Nagy, G. Subklew, H. Schlimper, M. Schwuger, J. Adsorption 2 (1996) 81.
[43] A. Guinier, G. Fournet, Small Angle Scattering of X-Rays, Wiley, New York, 1955.
[44] S.J. Gregg, K.S.W. Sing, Adsorption, Surface Area, and Porosity, Academic Press, New York, 1982.
[45] H. Kuwabara, T. Suzuki, K. Kaneko, J. Chem. Soc., Faraday Trans. 87 (1991) 1915.
[46] H.P. Boehm, E. Diehl, W. Heck, R. Sappok, Angew. Chem., Int. Ed. Engl. 3 (10) (1964) 669.
[47] H.P. Boehm, Angew. Chem., Int. Ed. Engl. 5 (6) (1966) 533.
[48] K. Kinoshita, Carbon. Electrochemical and Physicochemical Properties, Wiley, New York, 1988, p. 105.
[49] M.T. Coltharp, N. Hackerman, J. Colloid Interface Sci. 43 (1973) 176.
[50] G. Schay, L.Gy. Nagy, J. Chim. Phys. (1961) 149.
[51] A. Dabrowski, M. Jaroniec, J. Colloids Surf. 73 (2) (1980) 475.
[52] M.T. Coltharp, N. Hackerman, J. Colloid Interface Sci. 43 (1973) 185.
[53] A.J. Groszek, G.I. Andrews, in: Third Conf. on Industrial Carbons and Graphite, Society of Chemical Industry, London, 1971, p. 156.
[54] A.J. Groszek, in: D.H. Everett (Ed.), Proc. Int. Symp. on Surface Area Determination, Butterworths, London, 1969, p. 313.
[55] P.N. Cheremishinoff, F. Eclerbusch (Eds.), Carbon Adsorption Handbook, Ann Arbor Science Publishers, Michigan, 1978.
[56] CRC Handbook of Chemistry and Physics, CRC Press, Boca Raton, FL, 63rd edn., 1983.
[57] A.L. McClellan, H.F Harnsberger, J. Colloid Interface Sci. 23 (1967) 577.
[58] H.F. Stoeckli, L. Ballerini, S. De Bernardini, Carbon 27 (1) (1989) 501.
[59] S.S. Barton, J. Colloid Surf. Sci. 158 (1993) 64.
[60] C.H. Tessmer, R.D. Vidic, L.J. Uranowski, Environ. Sci. Technol. 31 (1997) 1872.
[61] L. Noszkó, A. Bóta, Á. Simay, L.Gy. Nagy, Per. Polytech. 28 (1984) 293.
[62] A. Bóta, J. Valyon, K. László, L.Gy. Nagy, Per. Polytech. 41 (1) (1997) 25.
[63] G. Schay, L.G. Nagy, in: Recent Advances in Chemistry, vol. 18, Akadémiai Kiadó, Budapest, 1974, pp. 71–72.
[64] K. László, A. Bóta, L.G. Nagy, C.B. Frischkorn, Carbon 35 (5) (1997) 593.
[65] A. Bóta, K. László, L.G. Nagy, T. Copitzky, Langmuir 13 (1997) 6502.
[66] C.G. Shull, L.C. Roess, J. Appl. Phys. 18 (1947) 295.
[67] K.S.W. Sing, Pure Appl. Chem. 54 (1982) 2201.
[68] M.M. Dubinin, Progr. Surf. Membr. Sci. 9 (1975) 1.
[69] H. Marsh, B. Rand, J. Colloid Interface Sci. 33 (1970) 101.
[70] T.I. Izotova, M.M. Dubinin, Zh. fiz. khimii 39 (1965) 2796.
[71] J. Garrido, A. Linares-Solano, J.M. Martin-Martinez, M. Molina-Sabio, F. Rodriguez-Reinoso, R. Torregrosa, Langmuir 3 (1987) 76.
[72] F. Ehrburger-Dolle, M. Holz, J. Lahaye, Pure Appl. Chem. 65 (10) (1993) 2223.
[73] M.M. Dubinin, H.F. Stoeckli, J. Colloid Interface Sci. 75 (1) (1980) 34.
[74] Z. Spitzer, V. Bíba, O. Kadlec, Carbon 14 (1976) 151.
[75] M.M. Dubinin, Carbon 27 (1989) 457.
[76] B. McEnaney, Carbon 25 (1987) 69.
[77] H.F. Stoeckli, F. Kraehenbuehl, L. Ballerini, S. De Bernardini, Carbon 27 (1) (1989) 125.
[78] M.M. Dubinin, Carbon 23 (1985) 593.
[79] M.M. Dubinin, Pure Appl. Chem. 61 (11) (1989) 1841.
[80] J.H. de Boer, J.F. Custers, Z. Phys. Chem. 25 (1934) 225.
[81] F. London, Z. Phys. Chem. 11B (1931) 246.
[82] J.T. Cookson Jr., in: P.N. Cheremisinoff, F. Ellerbusch (Eds.), Carbon Adsorption Handbook, Ann Arbor Science, Ann Arbor, MI, 1978, p. 270.
[83] J.J. Kipling, Adsorption from Solutions of Non-Electrolytes, Academic Press, London, 1965, chapter 4.
[84] G.C. Gasser, J.J. Kipling, in: Proc. Fourth Conf. on Carbon, Pergamon Press, New York, 1960, p. 55.
[85] G. Schay, L.Gy. Nagy, J. Chim. Phys. (1961) 149.
[86] I. Dékány, Á. Zsednai, Z. Király, K. László, L.G. Nagy, Colloids Surf. 19 (1986) 47.
[87] I. Dékány, Á. Zsednai, K. László, L.G. Nagy, Colloids Surf. 23 (1987) 41.
[88] I. Dékány, T. Ábrahám, L.G. Nagy, K. László, Colloids Surf. 23 (1987) 57.
[89] J. Rudling, E. Björkholm, Am. Ind. Hyg. Assoc. J. 47 (1986) 615.
[90] G. Horváth, K. Kawazoe, J. Chem. Eng. Jpn. 16 (6) (1983) 470.
[91] L.R. Snyder, Principles of Adsorption Chromatography, Marcel Dekker, New York, 1968.